926–935 Nucleic Acids Research, 2011, Vol. 39, No. 3 Published online 28 September 2010
doi:10.1093/nar/gkq826

Single-strand nicks induce homologous recombination with less toxicity than double-strand breaks using an AAV vector template

Michael J. Metzger[1,2], Audrey McConnell-Smith[2,3], Barry L. Stoddard[3] and A. Dusty Miller[1,*]

[1]Human Biology Division, Fred Hutchinson Cancer Research Center, Seattle, WA 98109, [2]Graduate Program in Molecular and Cellular Biology, University of Washington, Seattle, WA 98195 and [3]Basic Sciences Division, Fred Hutchinson Cancer Research Center, Seattle, WA 98109, USA

Received July 22, 2010; Revised August 28, 2010; Accepted September 2, 2010

ABSTRACT

Gene targeting by homologous recombination (HR) can be induced by double-strand breaks (DSBs), however these breaks can be toxic and potentially mutagenic. We investigated the I-AniI homing endonuclease engineered to produce only nicks, and found that nicks induce HR with both plasmid and adeno-associated virus (AAV) vector templates. The rates of nick-induced HR were lower than with DSBs (24-fold lower for plasmid transfection and 4- to 6-fold lower for AAV vector infection), but they still represented a significant increase over background (240- and 30-fold, respectively). We observed severe toxicity with the I-AniI 'cleavase', but no evidence of toxicity with the I-AniI 'nickase.' Additionally, the frequency of nickase-induced mutations at the I-AniI site was at least 150-fold lower than that induced by the cleavase. These results, and the observation that the surrounding sequence context of a target site affects nick-induced HR but not DSB-induced HR, strongly argue that nicks induce HR through a different mechanism than DSBs, allowing for gene correction without the toxicity and mutagenic activity of DSBs.

INTRODUCTION

The strategy of altering a gene at its endogenous locus ('gene correction') rather than adding a new gene ('gene addition') has the potential to solve many problems in gene therapy, such as insertional mutagenesis by integrated transgenes and loss of non-integrated transgenes, as well as silencing and inappropriate regulation. Previous work has shown that efficient homologous recombination (HR) can be achieved both in cell culture and *in vivo* by the use of an adeno-associated virus (AAV) vector to deliver a repair template (1,2). And just as double-strand breaks (DSBs) have been shown to induce HR with a transfected template (3,4), it has also been shown that DSBs induced by homing endonucleases at specific target sites increase the rate of HR with an AAV repair template by 60- to 100-fold (5,6).

DSBs induced by homing endonucleases can lead to problems, however. Breaks that are not repaired using the homologous template may be predominantly repaired via a non-homologous end-joining (NHEJ) pathway—a process that can cause base pair insertions, deletions, mutation or chromosomal translocation. This represents a significant concern for therapeutic applications, especially given the recent demonstration that the I-SceI homing endonuclease (which has a long history of gene targeting applications) displays a measurable amount of off-target cleavage activity (7). Even at a DNA location that is specifically targeted for templated repair, NHEJ can effectively compete with HR, rendering the site resistant to future cleavage and therefore resistant to future repair. After only 2 days of expression of I-SceI in cells, I-SceI sites resistant to *in vitro* cleavage (due to inaccurate repair of the DSB) can be detected by Southern blotting (5).

Evidence from several studies has suggested that nicks may also induce HR. In the mating type switch of fission yeast at the *mat1* locus, there is evidence that a single-strand nick initiates the gene conversion switching event (8). Other studies have shown that nicks or single-strand lesions can induce meiotic recombination as well as V(D)J and Ig V recombination (9–12). Additionally, a recent study used the AAV Rep protein to induce HR at the AAVS1 site using a plasmid repair template (13). Rep

*To whom correspondence should be addressed. Tel: +1 206 667 2890; Fax: +1 206 667 6523; Email: dmiller@fhcrc.org

protein is known to nick the AAVS1 site in human cells; however, Rep has helicase and ATPase activity (and has been shown to be toxic in cells and produce genomic rearrangements at the AAVS1 site as well), so the implications of this study on nick-induced HR are unclear (14,15). Additionally, while well-described homing endonucleases, including enzymes from the LAGLIDADG family such as I-SceI, I-CreI and I-AniI, induce homing through DSBs, some phage-derived homing endonucleases, such as I-HmuI and I-HmuII, induce homing by initially generating nicks (16,17).

A generalized strategy, involving mutation of an active site lysine, has been described by two separate laboratories to create site-specific nicking enzymes ('nickases') from both the I-SceI and I-AniI LAGLIDADG homing endonucleases (18,19). In the latter example, the generation of the K227M mutation in I-AniI was shown to produce an endonuclease scaffold with a DNA-binding affinity, strand cleavage mechanism and specificity profile that was similar to the parental wild-type enzyme. This construct allows for the direct comparison of the effects of single-strand nicks to DSBs while keeping every other aspect of the HR assay constant, including target design, recognition sequence and the method of delivery of the endonuclease—the only difference being a single residue in the endonuclease active site, and the resulting formation of a nick, rather than a DSB, at the DNA target site (19). In this study, we investigated the ability of this nickase to induce HR using both plasmid and AAV templates. We find that the nickase induces HR with both types of template with far lower toxicity than that induced by DSBs and found evidence that the nicks induce HR through a mechanism that is distinct from that of DSBs.

MATERIALS AND METHODS

Tissue culture

Human embryonic kidney 293 and 293T cells were grown in Dulbecco's modified Eagle medium (DMEM) plus 10% Cosmic Calf Serum (Thermo Scientific) at 37°C in a 10% CO_2 atmosphere.

Plasmid construction

Target plasmids pCnZPNOA2 and pCnZPNOA3 were generated by site-directed mutagenesis of pCnZPNO (gift of Dan Miller and David Russell, University of Washington) using primers AnidE2F and AnidE2R (cgctgatcctttgcTTACAGAGAAACCTCCTCAtacgcccacg cgatg and its complement) for pCnZPNOA2 and AnidE3F and AnidE3R (gctgatccttTTACAGAGAAAC CTCCTCAtgggtaacagtcttg and its complement) for pCnZPNOA3. Plasmid pExodusY2 (expressing an HA-tagged nuclear localized DSB-inducing I-AniIY2 in a pcDNA3.1 backbone) and lentivirus construct pRRLsinExY2imC (expressing an HA-tagged DSB-inducing I-AniIY2 and mCherry with the full name pRRLSIN.SFFV.HA.2ndGenNLS.reoAniY2.IRES.mC-herry) were a gift from Mike Certo and Andrew Scharenberg (Seattle Children's Research Institute). The K227M nicking variants (pnExodusY2 and pRRLsinnExY2imC) were generated using site-directed mutagenesis with primers nExodusK227M-F and nExodusK227M-R (gttaggcaacATGaaactgcaatac and its complement) and the K227M/E148Q catalytically inactive variants (pdExodusY2 and pRRLsindExY2imC) were generated using the above primers as well as dExodusE148Q-F and dExodusE148Q-R (gatttatag aagctCAGggctgtttcag and its complement). Empty lentivirus vector pRRLsinXimC was generated by removing an RsrII/SbfI fragment containing the I-AniIY2 gene from pRRLsinExY2imC.

Generation of target cells

The foamy virus vectors used to insert the inactive *lacZ* target containing an I-AniI recognition site were generated by transfection of 293T cells with foamy virus production plasmids pCINGSΔΨ, pCINPS and pCINES (20) (gifts of Dan Miller and David Russell, University of Washington) and foamy virus vectors pCnZPNOA2 or pCnZPNOA3. Vector-containing culture medium was collected and filtered (0.45 μm pore size). Polyclonal populations of target cells were generated by seeding 293 cells at 2.5×10^5 cells per 6-cm dish and transducing the cells with the foamy virus vectors the next day. Two days post-transduction, cells were trypsinized and seeded into medium containing 400 μg/ml G418 for selection of transduced cells. Each polyclonal population was a mixture of 50–200 clones with different vector integration sites.

Transfection HR assay

Target cells (293/CnZPNOA2 and 293/CnZPNOA3) were seeded at 2×10^6 cells per 6-cm dish on Day 0 and transfected on Day 1 with 5 μg of the *lacZ* repair template plasmid (pA2nZ3113) and 5 μg of one of the I-AniI expression plasmids (pExodusY2, pnExodusY2, pdExodusY2 or pLXL-gfp as a control) per 6-cm dish. The medium was changed on Day 2 and cells were fixed and stained for β-gal expression on Day 3. Values presented are β-gal$^+$ cells/cm^2 for confluent 6-cm dishes.

Generation of lentivirus vectors

293T cells were transfected with lentivirus production plasmids (pMDG and pCMVΔR8.2) (21) and one of the I-AniI expression vectors (pRRLsinExY2imC, pRRLsinnExY2imC, pRRLsindExY2imC or empty vector pRRLsinXExY2imC). Vector-containing culture medium was collected and filtered (0.45 μm pore size). To titer virus, 293 cells were seeded at 5×10^4 cells/well of 24-well plates. Cells were transduced with 20 μl of each virus the next day and titer was determined by quantification of mCherry-expressing cells using flow cytometry 2 days after transduction.

Quantitative PCR

For each reaction, 500 ng of genomic DNA were digested overnight *in vitro* with purified I-AniIY2 (at 0.5 nM) before amplification. Primer pairs lacZqF1 (GCGTTAA

CTCGGCGTTTCAT), lacZqR1 (GCGCTCAGGTCAA ATTCAGAC) and lacZqF2 (CCCGGCTGTGCCGAA ATGGT), lacZqR2 (CCGACCACGGGTTGCCGTTT) were used with Maxima SYBR Green kit (Fermentas) in triplicate for each data point. A standard curve was generated with 10-fold dilutions of plasmid CnZPNOA3 (linearized with SpeI) from 10^6 to 10 copies per reaction. Each standard value was done in triplicate for both primer sets and all genomic DNA values fell within this linear standard curve. Products of qPCR reactions were digested overnight *in vitro* with I-AniIY2 (at 0.375 nM) and visualized with ethidium bromide on an agarose gel. ImageJ was used to quantify the fraction of the qPCR product that was not cut by I-AniIY2.

Production of the AAV vector template for HR

AAV vectors were produced by seeding 4×10^6 293 cells per 10-cm dish and transfecting the next day with the AAV2 production plasmid pDG and AAV vector plasmid pA2nZ3113 (20 and 10 μg per dish, respectively). Cells and culture medium were collected and the AAV vector was purified using heparin columns as described earlier (22). Vector quantification was done by Southern blot of DNA extracted from the purified vector preparations.

AAV HR assay and titration of I-AniI toxicity

On Day 0, 5×10^4 target cells per well were seeded in 24-well dishes and were transduced with one of the I-AniI-expressing lentivirus vectors on Day 1. On Day 3, 5×10^4 lentivirus-transduced cells were seeded into wells of a new 24-well dish, and AAV2-nZ3113 was added on Day 4. On Day 5, 0.25% of the cells from each well were seeded in 10-cm dishes to measure the number of viable cells, and 99.75% of cells were seeded in 15-cm dishes to measure HR. Medium was changed on Day 9. On Day 13, cells in the 10-cm dishes were fixed and surviving colonies were counted after Coomassie staining, and cells in the 15-cm dishes were fixed and stained for β-gal expression. Total β-gal$^+$ foci (clusters of two or more β-gal$^+$ cells) were counted.

In vitro cleavage and nicking assays

Digests were conducted using purified I-AniIY2 cleavase and I-AniIY2 nickase (19) at 37°C in 10 mM $MgCl_2$, 100 mM NaCl, 50 mM Tris–HCl, pH 7.5 using 10 nM of either pnZBA2 or pnZBA3 plasmid (generated from the 5.7-kb BamHI fragments from pCnZPNOA2 and pCnZPNOA3, respectively, which include the entire *lacZ* gene containing the I-AniI recognition site), and reactions were stopped with 2 × stop solution described earlier (19). Supercoiled, nicked and linear plasmid DNA was detected on a 1% agarose gel and quantified using ImageJ.

Statistical analysis

All statistical analyses comparing CnZPNOA3 and CnZPNOA2 targets used a paired, one-tailed Student's *t*-test.

RESULTS

Nicks induce HR with a transfected template

The HR-inducing ability of the I-AniI nickase was first determined by transfecting cells with a plasmid repair template and an I-AniI expression plasmid (Figure 1). In all experiments, the I-AniI nickase, cleavase and inactive enzyme are in the context of an otherwise identical 'Y2' I-AniI scaffold, which harbors two point mutations (S111Y and F13Y) previously identified in a screen for enhanced *in vivo* enzymatic activity (23). Target cells were a polyclonal population of 293 cells transduced with a foamy virus vector containing a nuclear localized *lacZ* target inactivated by the addition of the I-AniI recognition site at a position encoding a catalytically required residue (293/CnZPNOA3 cells). These cells do not express β-gal unless the *lacZ* gene is repaired. Cells transfected with the template plasmid but with no I-AniI expression plasmid showed very low numbers of β-gal-expressing cells 2 days after transfection, demonstrating very inefficient HR in the absence of an endonuclease (Figure 1B). Similar low levels were seen with a catalytically inactive I-AniI expression plasmid. In contrast, the cleavase induced a 5900-fold increase relative to cells transfected with template but no endonuclease. Expression of the nickase also produced a significant 240-fold increase in β-gal repair, although this level is 24-fold less than that seen with DSBs. These data confirm the previous results that the nicking variant of I-AniI can indeed induce HR with a transfected template at a significant rate, but they do not indicate whether the nicks that induce HR are first

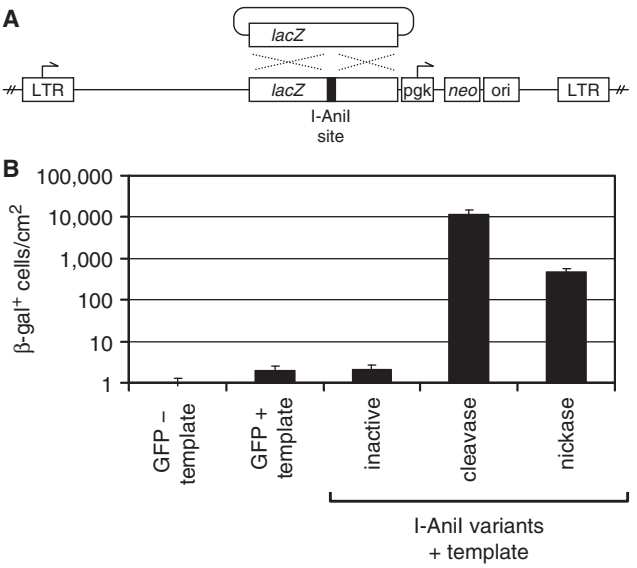

Figure 1. Nicks induce HR with a transfected template. (**A**) Schematic of integrated target site CnZPNOA3, with a *lacZ* gene inactivated by the introduction of the I-AniI recognition site (black box). The repair template plasmid (pA2nZ3113) is shown above with regions of homology indicated by a dotted 'X'. (**B**) β-gal$^+$ cells per cm^2 in confluent polyclonal 293/CnZPNOA3 cells transfected with one of the plasmids expressing either GFP or the inactive, cleavase or nickase I-AniI and template plasmid pA2nZ3113 (except for the GFP−template condition, in which cells were transfected with only GFP-expressing plasmid). Values are means of four experiments ± SE.

converted to DSBs or induce HR through a different mechanism (19).

Detection of DSBs and mutations in cells expressing I-AniI cleavase and nickase

After confirming that the nickase can induce HR, we next investigated the generation of DSBs in cells expressing the I-AniI cleavase or the nickase. 293/CnZPNOA3 cells were transduced with equivalent levels of lentiviral vectors containing each of the I-AniI expression constructs at a multiplicity of infection (MOI) of one transducing unit per cell (TU/cell), based on titers established by vector expression of mCherry. Genomic DNA was extracted after 3 days and Southern analysis showed DSBs at 10% of the target sites in cells expressing the cleavase, but no evidence of DSBs in nickase-expressing cells (Figure 2B, lanes labeled SpeI).

In addition to observing the fraction of sites cleaved in transduced cells, we also investigated the fraction of I-AniI sites that had been rendered resistant to *in vitro* I-AniI cleavage due to mutations at the I-AniI site (Figure 2B, lanes labeled SpeI + I-AniIY2). At only 3 days after transduction of cells with cleavase-expressing lentivirus, 20% of the target sites could not be cleaved by digestion with I-AniI *in vitro*. In contrast, no evidence of mutation was observed in parallel experiments conducted with the nickase. Additionally, no evidence of mutation was observed with nickase at an MOI of 2 TU/cell, while the 4.0-kb band indicative of mutation was clearly observed in cells transduced with cleavase at an MOI of 0.25 TU/cell (data not shown). Equivalent levels of expression of all three I-AniI variants from lentiviral vectors at an MOI of 1 TU/cell were confirmed by western analysis (Figure 2C). Thus, while the DSB-inducing cleavase was highly active at the integrated target site in the 293/CnZPNOA3 cells, no detectable evidence of DSBs was observed following expression of nickase.

Because the nickase induced HR with a transfected template at a rate 24-fold less than the cleavase, this could be explained through a DSB-mediated process if the nickase generated DSBs at a rate 24-fold less than cleavase. Therefore, we developed a qPCR-based assay to more sensitively detect potential DSB-induced mutations. Genomic DNA from cells transduced with endonuclease-expressing lentivirus was digested *in vitro* with I-AniI as with the Southern assay, but this DNA was then used as a template for qPCR. Two primer pairs were used. Primer pair 1 (lacZqF1/lacZqR1) amplifies a region 5′ of the I-AniI site, while primer pair 2 (lacZqF2/lacZqR2) flanks the I-AniI site (Figure 3A). After digestion with I-AniI *in vitro*, naïve target sites will be cut and are not amplified by pair 2, whereas mutated sites will not be digested and will be amplified. Thus, the ratio of amplification of primer pair 2 to that of pair 1 estimates the frequency of mutation by NHEJ, assuming 100% *in vitro* cleavage by I-AniI. In agreement with the Southern analysis, the frequency of uncleavable sites in cleavase-transduced cells was 30% (Figure 3B).

To determine whether the products amplified were, in fact, mutated, or whether they represent amplification

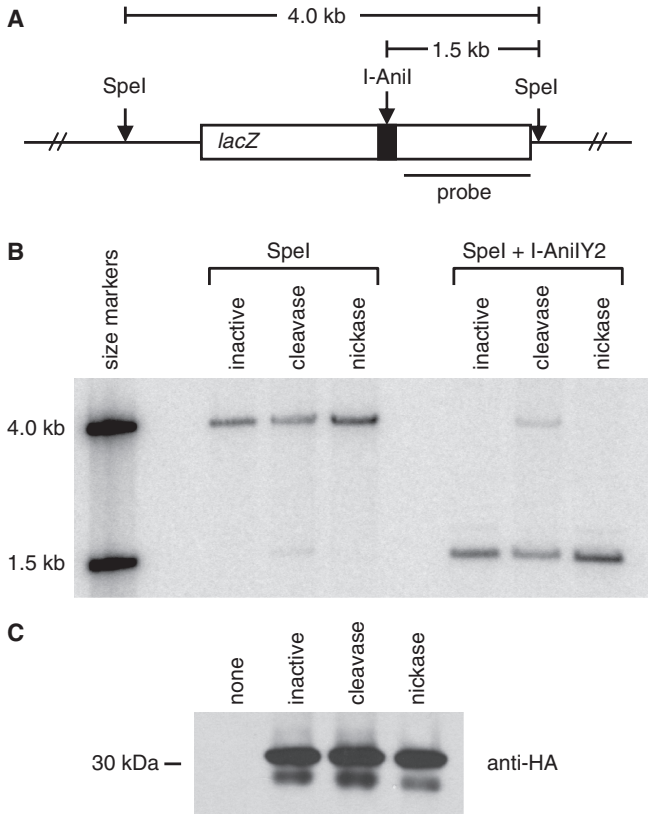

Figure 2. Expression of I-AniI cleavase generates DSBs, but nickase does not. (**A**) Schematic of the integrated target site CnZPNOA3, containing the I-AniI recognition site, with probe and enzyme cleavage sites marked. (**B**) Genomic DNA was extracted from 293/CnZPNOA3 cells 3 days after transduction with I-AniI-expressing lentivirus—either inactive, cleavase or nickase. DNA was digested *in vitro* with either SpeI alone or SpeI and purified I-AniI cleavase before being used for the Southern blot. Size markers were generated by *in vitro* digestion of pCnZPNOA2 plasmid with SpeI and SpeI/I-AniI and gel extraction of 4.0- and 1.5-kb bands, respectively. (**C**) Cell lysate was collected from 293/CnZPNOA3 cells 3 days after transduction with the same I-AniI-expressing lentivirus preparations used for the Southern blot and further HR assays. An amount of 10 μg of each lysate was loaded for western analysis and anti-HA antibody (mouse mAb 6E2, Cell Signaling Technology) was used to detect the HA-tagged I-AniI proteins.

of naïve I-AniI sites which were intact due to incomplete digestion, the products of the initial qPCR reaction were digested and analyzed by ethidium bromide on an agarose gel (Figure 3C). No detectible I-AniI digestion of the amplified product was observed from cleavase-expressing cells, suggesting amplification of true NHEJ-mutated sites. However, the majority of the product from nickase and inactive endonuclease-expressing cells was digested, showing that the observed qPCR amplification was due to incomplete digestion prior to the qPCR. By multiplying the ratio of primer pair two to one times the fraction of the qPCR product that remains intact after further digestion, we can generate a more sensitive estimate of NHEJ mutation at the I-AniI site. This suggests that the nickase may generate some NHEJ mutations at the I-AniI site, but this mutation rate was at least 150-fold lower than that with cleavase, when the

A

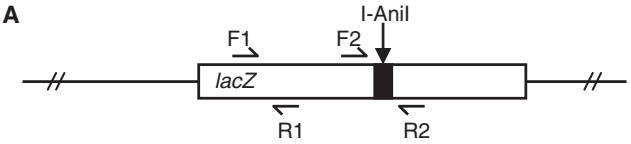

B

I-AniI	Ratio of primer pair 2: primer pair 1	Uncleavable fraction of qPCR product	Estimate of NHEJ (%)
none	0.0032	0.19	0.065
inactive	0.0071	0.14	0.099
cleavase	0.30	0.98	30
nickase	0.012	0.17	0.21

C

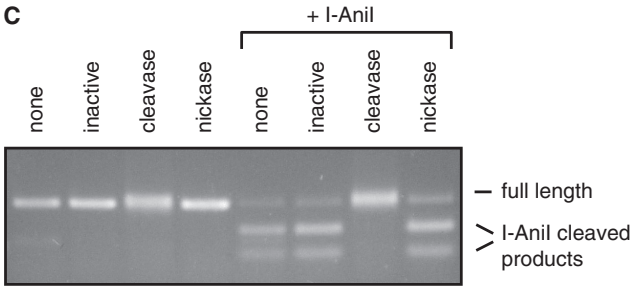

Figure 3. Analysis of potential NHEJ mutations using a sensitive qPCR-based assay. (**A**) Schematic of the integrated target site CnZPNOA3 showing the positions of the primers used for qPCR: lacZqF1 (F1), lacZqR1 (R1), lacZqF2 (F2) and lacZqR2 (R2). (**B**) Table showing the ratio of qPCR amplification with primer pair 2 to primer pair 1 after digest of genomic DNA with I-AniI, analysis of the fraction of the qPCR products which cannot be cleaved by I-AniI, and the final estimated percentage of mutated I-AniI sites (a product of the first two columns). Values are means of two experiments calculated independently (individual values for nickase-induced mutation were 120- and 180-fold less than that with cleavase). (**C**) Primer pair 2 qPCR products were digested with I-AniI, and a representative agarose gel revealing the digested and undigested products is shown.

enzymes were expressed at equivalent levels for 3 days. Since the HR-induction of the nickase was only 24-fold less than cleavase, this argues that a low rate of DSB-generation by the nickase cannot account for the observed nickase-induced HR.

Nicks induce HR with an AAV-delivered template

To determine the ability of nicks to induce HR with an AAV-delivered template, we established a 13-day assay based on previous protocols that measures cell survival as well as HR (5). Polyclonal 293/CnZPNOA3 cells described above were transduced (Day 1) with I-AniI-expressing lentivirus vectors at varying MOIs to provide long term enzyme expression. Cells were trypsinized and replated on Day 3 and were infected on Day 4 with the AAV2-nZ3113 template. Cells were trypsinized and replated again on Day 5, and on Day 13 cells were stained for β-gal expression (99.75% of cells) and for colony formation using Coomassie blue stain (0.25% of cells).

The first result we observed was that long-term expression of I-AniI cleavase resulted in severe toxicity in target cells that greatly affected the amount of HR observed (Figure 4C). When cells were transduced with an MOI of 1 TU/cell, cell death was consistently >80%, and a clear dose-response effect was seen with increasing DSBs. Toxicity was not noticeable until about 3–5 days after transduction, which explains why this phenomenon was not seen in previous 2-day transfection assays. In contrast, no significant toxicity was detected with the nickase up to an MOI of 1 TU/cell. Some toxicity was observed with nickase at MOIs >1 TU/cell; however, similar levels of toxicity were observed with the catalytically inactive enzyme, so the observed minor toxicity is not likely to be due to the enzymatic activity of the nickase. In addition, a 'blank' lentivirus vector expressing only mCherry showed similar toxicity, suggesting that the toxicity is likely due to transduction with the lentivirus vector rather than expression of endonuclease (data not shown). Also, to investigate long-term toxicity, we followed the mCherry expression over time of cells transduced with the lentivirus vectors at an MOI of 0.25 TU/cell. While we again found evidence of some lentivirus-induced toxicity, we found no difference in the survival of cells transduced with the nickase-expressing and inactive enzyme-expressing lentivirus vectors for >30 days in a dividing population, while cleavase-expressing cells continued to exhibit decreased survival over time until undetectable in the population (Supplementary Figure S1).

Increasing the amount of DSBs at the target site did increase the amount of β-gal$^+$ foci, but a sharp decrease was observed at MOIs >0.5 TU/cell, concomitant with the drop in survival (Figure 4B). The nickase enzyme induced significant levels of HR using the AAV template and HR rates increased with increasing amounts of enzyme. The toxicity of DSBs makes a direct comparison of HR-inducing activity difficult. More HR foci were observed with DSBs than with nicks at an MOI of 1 TU/cell, but more foci were observed with nicks than with DSBs at an MOI of 4. Because the amount of HR observed with nicks at an MOI of 1 TU/cell was equivalent to that observed with DSBs at an MOI of 0.125 we can estimate that 8-fold more nickase expression is required for equivalent amounts of HR with an AAV template.

We next wanted to determine if the amount of HR observed above with an AAV vector MOI of 1.5×10^4 vg/cell represented a maximum, or whether increasing the amount of available AAV template could increase the rate of HR. Using a constant amount of I-AniI-expressing lentivirus, we observed a clear dependence of HR on the amount of AAV template (Figure 4D). With both nicks and DSBs, HR increased with no evidence of saturation at any of the AAV MOIs used, yielding a maximum of 61 and 249 β-gal$^+$ foci, respectively. With 1.5×10^4 to 1.5×10^5 AAV vg/cell, DSB-induced HR was only 4- to 6-fold greater than nick-induced HR. Because only two foci of HR were observed in the absence of any endonuclease with the highest amount of AAV template, we can estimate that the presence of DSBs

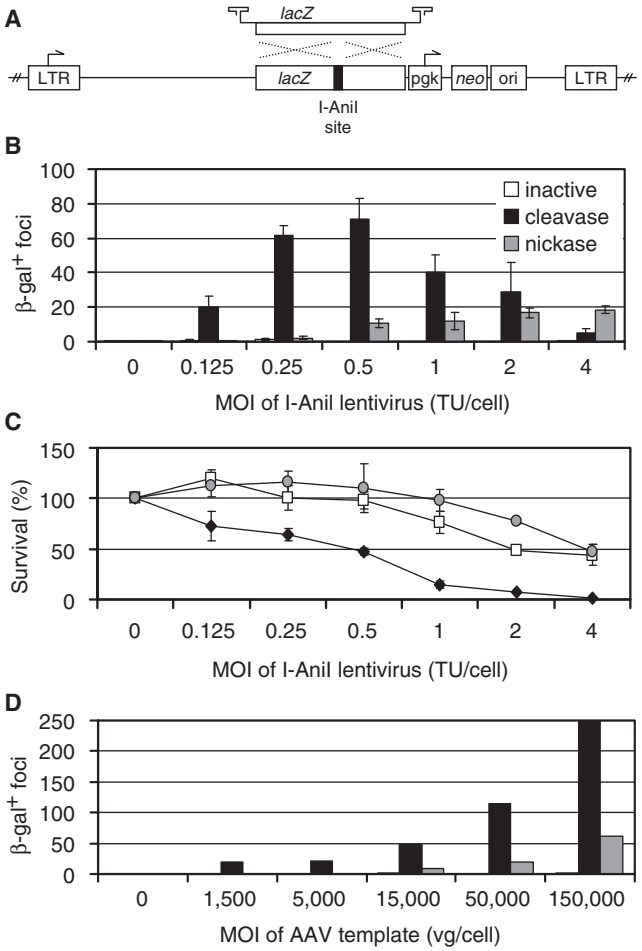

Figure 4. Nicks induce HR with an AAV vector template with less toxicity than DSBs. (**A**) Schematic of integrated target site CnZPNOA3, with a *lacZ* gene inactivated by the introduction of the I-AniI recognition site. The AAV2-nZ3113 genome used as an HR template is shown above with homology indicated by a dotted 'X'. (**B**) β-gal$^+$ foci counted 9 days after infection of 5×10^4 cells with 1.5×10^4 vg/cell AAV2-nZ3113. Cells were transduced with different MOIs of the three I-AniI-expressing lentivirus vectors 3 days prior to AAV vector delivery. (**C**) Survival of cells transduced with different MOIs of the three I-AniI-expressing lentivirus vectors determined by counting Coomassie-stained colonies 9 days after AAV vector infection and normalized to colony-forming ability of untransduced cells assayed in parallel. Survival points and β-gal$^+$ bars represent means of three experiments ± SE, each conducted with independent polyclonal cell populations. White bars and white squares represent inactive I-AniI-expressing lentivirus; black bars and black diamonds, I-AniI cleavase; gray bars and gray circles, I-AniI nickase. (**D**) β-gal$^+$ foci counted 9 days after infection of 5×10^4 cells with varying amounts of AAV2-nZ3113. All cells were transduced with I-AniI-expressing lentivirus vectors 3 days earlier at an MOI of 1 TU/cell. White bars represent mock-lentiviral infection; black bars, cleavase; gray bars, nickase.

increased the HR rate about 100-fold and nicks increased the rate 30-fold.

Optimal timing of endonuclease delivery for HR

In the protocol above, we transfected cells with endonuclease-expressing lentivirus 3 days before exposing cells to the AAV template to make sure the enzyme was expressed prior to infection. We also wanted to test the effect of timing of endonuclease and template delivery, as this parameter might be critical in determining the optimal delivery of the two components in any therapeutic protocol. The nickase generated a significant amount of β-gal$^+$ foci (57 and 60 foci in two experiments; Figure 5) when delivered 3 days prior to AAV infection, as done previously, whereas the high toxicity of the DSBs limited β-gal$^+$ foci to very low amounts. In contrast, when both the I-AniI-expressing lentivirus and AAV template were delivered at the same time, the level of HR from the cleavase was higher (Figure 5). One important note is that there were three fewer days for DSB-induced toxicity in this protocol; indeed, many of the β-gal$^+$ foci appeared to be clusters of small numbers of multinucleate cells that may not have survived three more days. Also, when expressed prior to AAV infection, the DSBs mutate a significant amount of the I-AniI target sites before the AAV template is available for recombination. No induction of HR was observed when the lentivirus was added 3 days after AAV, but it is unclear whether this was due to rapid uncoating of the AAV2 capsid or whether this was simply due to decreased lentiviral transduction efficiency in a sub-confluent 15-cm dish.

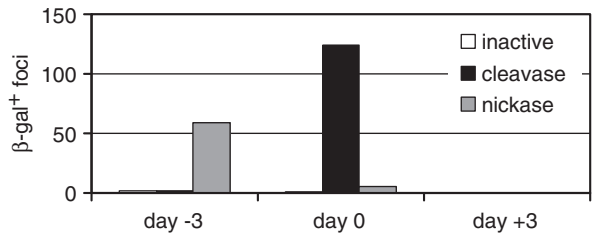

Figure 5. Timing of endonuclease delivery. β-gal$^+$ foci counted 9 days after infection of 293/CnZPNOA3 cells with 2×10^4 vg/cell of AAV2-nZ3113. In all cases, cells were seeded at 5×10^4 cells per well in 24-well plates the day before AAV vector infection. Cells were transduced with one of three I-AniI-expressing lentivirus vectors (at an MOI of 2.5 TU/cell) at three different times: 3 days before, the same time as, or 3 days after AAV vector infection. Results are means of two experiments, except for the transduction 3 days after AAV vector infection and the nickase transduction at the same time as AAV vector infection, which are means of three experiments. White bars represent inactive I-AniI-expressing lentivirus; black bars, I-AniI cleavase; gray bars, I-AniI nickase.

Interestingly, when both the I-AniI-expressing lentivirus and AAV template were delivered at the same time, the level of HR from the nickase was much lower than when the nickase was expressed prior to AAV delivery. We considered the possibility that the AAV template could have affected lentiviral transduction, but we found that the AAV vector had no effect on expression of mCherry from the lentiviral vector. These data suggest that, in contrast to DSBs, nicks may need to be generated prior to the addition of template, and perhaps nick-induction of HR requires epigenetic changes that occur after repeated nicking. In summary, these results show that timing of delivery of an endonuclease and a repair template can greatly affect the ability of the nick or break to induce HR.

Sequence context of the endonuclease target site affects nick-induced HR, but not DSB-induced HR

In addition to the CnZPNOA3 target described earlier, a second inactive *lacZ* target with an I-AniI recognition site was generated to determine if target design affected HR. In both targets, a catalytic residue (Glu 537) (24) was removed and the 19 bp I-AniI recognition sequence was added (Figure 6A). In the CnZPNOA3 target used above, termed the 'replacement' target, 19 bp of the *wt lacZ* gene surrounding the Glu codon were exactly replaced with the 19-bp I-AniI sequence. In the new CnZPNOA2 target, termed the 'insertion' target, only the Glu codon was removed and the 19-bp I-AniI sequence was inserted, generating a 16-bp insertion in the inactive reporter gene relative to the *wt* sequence. In both cases, the target site itself was exactly the same DNA sequence.

In the transfection assay, the rates of DSB-induced HR with the two targets were indistinguishable; however, there was a significant difference in nick-induced HR (Figure 6B). The amount of HR with the replacement target was 7.3-fold higher than that observed with the insertion target ($P = 0.005$). A similar effect was observed with the AAV-delivered template. The amounts of DSB-induced HR observed with replacement and insertion targets show no significant differences, but the amount of nick-induced HR was 5.5- to 12-fold higher with the replacement target at all MOIs $\geq$0.5 TU/cell (Figure 6C and D).

It was conceivable that differences in sequence flanking the 19-bp I-AniI recognition site could affect the behavior of the cleavase and nickase differently, and thus explain these divergent results. In particular, it has been reported that a 20th base pair can influence I-AniI catalytic activity (25). We therefore performed a control experiment, in which we assayed the kinetics of activity of purified I-AniI cleavase and nickase on plasmids containing the replacement and insertion targets *in vitro* and observed that both the cleavage and nicking rates of the two targets were very similar (Figure 7A, B, Supplementary Figure S2A and B). We also digested both targets with varying amounts of cleavase and nickase *in vitro* and determined that the replacement target was cleaved and nicked at slightly lower concentrations than the insertion target, but the ratio of cleavage to nicking was similar for both targets (Figure 7C, D, Supplementary Figure S2C and D).

Based on these data from two different template delivery mechanisms, the surrounding sequence context does not affect DSB-induced HR, but it does affect nick-induced HR by ~10-fold. These results cannot be explained by differences of enzyme activity at the different sequences, and argue that nick-induced HR proceeds through a different mechanism than DSB-induced HR.

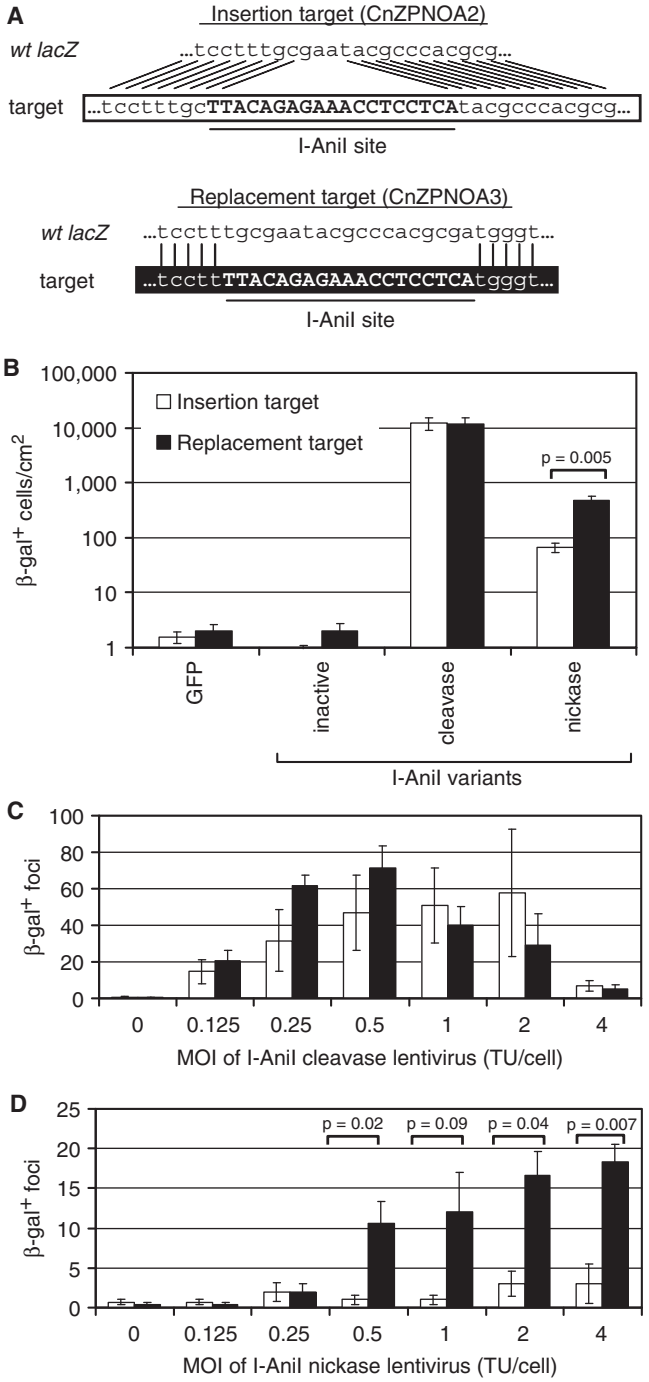

Figure 6. Target design affects nick-induced HR, but not DSB-induced HR. (**A**) Schematic of the differences between the insertion (CnZPNOA2) and replacement (CnZPNOA3) targets with homology to *wt lacZ*. The I-AniI recognition site is capitalized and in bold for both targets. (**B**) β-gal$^+$ cells/cm^2 after transfection as in Figure 2, using 293 cells with integrated insertion target (CnZPNOA2, white bars) or replacement target (CnZPNOA3, black bars). Means of four experiments ± SE. (**C**) β-gal$^+$ foci after transduction with cleavase-expressing lentivirus and infection with AAV2-nZ3113 as in Figure 3. Means of three experiments ± SE. (**D**) β-gal$^+$ foci after transduction with nickase-expressing lentivirus and infection with AAV2-nZ3113 as in Figure 3. Means of three experiments ± SE.

DISCUSSION

We have confirmed the previous report that a homing endonuclease engineered to generate single-strand nicks instead of DSBs does induce HR in cells transfected

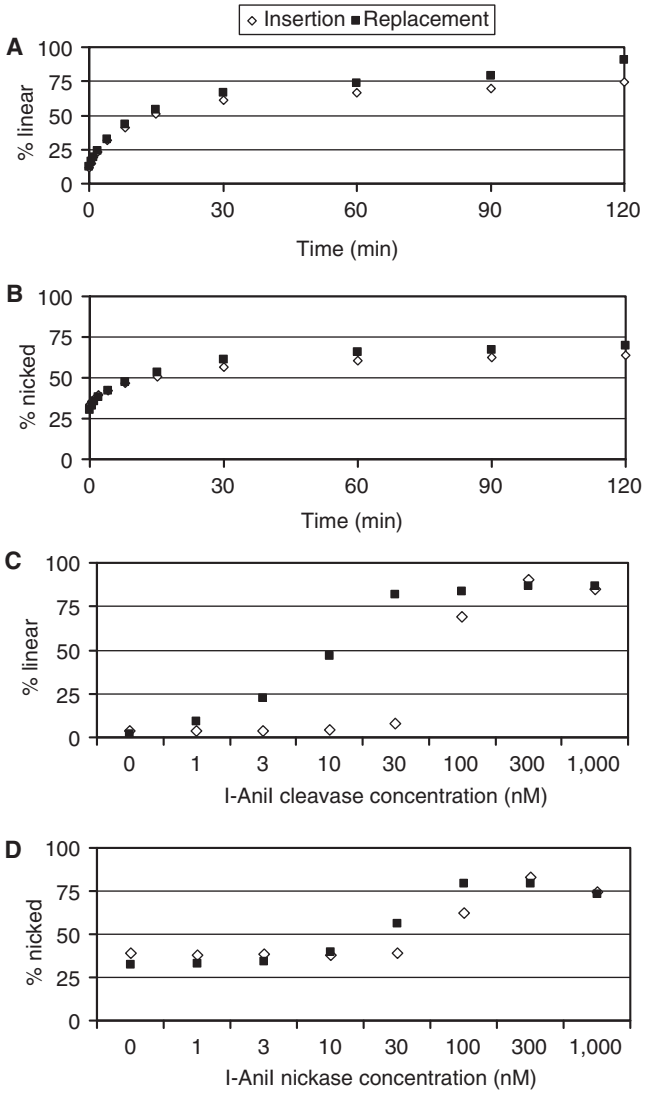

Figure 7. *In vitro* comparison of replacement and insertion targets. (**A**) Frequency of linearized plasmid containing either the insertion target (pnZA2, white diamonds) or replacement (pnZA3, black squares) following *in vitro* digestion with 1 μM purified I-AniI cleavase at 37°C for 0–2 h. (**B**) Frequency of nicked plasmids with 1 μM purified I-AniI nickase. (**C**) Frequency of linearized plasmid with both targets with increasing concentrations of purified I-AniI cleavase for 2 h at 37°C *in vitro*. (**D**) Frequency of nicked plasmid with increasing concentrations of purified I-AniI nickase for 2 h at 37°C *in vitro*.

with a plasmid repair template (19), and we demonstrated for the first time that a nicking endonuclease can induce HR with an AAV vector-delivered template. Nicks induced HR with an AAV template at a rate only 4- to 6-fold less than DSB-induced HR when equivalent amounts of enzyme were expressed. In addition, we showed that DSBs generated by a homing endonuclease have severe toxicity in cell culture assays lasting longer than 2 days. Nicks showed no evidence of toxicity, and showed no evidence of DSBs or NHEJ mutation products by Southern analysis. A more sensitive analysis indicates that expression of nickase generates mutations at a rate that is at least 150-fold lower than does the cleavase. This argues that the HR-inducing ability of the nickase cannot be explained by DSBs. These results suggests that other nicking endonucleases, such as the nicking I-SceI (18), could be useful in inducing HR in a broad array of gene correction applications with less toxicity than DSBs.

With the highest amounts of AAV template used in these assays, we observed 61 β-gal$^+$ foci in 5×10^4 infected cells, for an absolute rate of 0.12%. However, no evidence of any threshold of HR activity was observed, so it is likely that higher HR will be observed with higher MOIs of AAV template and with greater expression of nickase. In addition, this rate reflects a 30-fold increase over the rate of HR in the absence of nicks.

In this study, rates have been represented as HR foci per AAV-treated cell rather than HR foci per surviving cell. When presented per surviving cell, the DSBs appear to induce HR at a higher rate, but this obscures their severe toxicity. This might be acceptable in an *ex vivo* protocol, but toxicity upwards of 90% would clearly be unacceptable for most *in vivo* applications. The use of DSBs for *ex vivo* clinical protocols also assumes that the surviving cells are not damaged in any way, and this is unlikely. In addition to the observed acute cell death there are likely other affects on the cell such as potentially oncogenic translocations and DNA damage that could impair the cell or cause death after a longer period of time as demonstrated by the continued toxicity of DSBs in a long-term survival assay (Supplementary Figure S1).

Our results show that design of the target site greatly affects nick-induced HR, but not DSB-induced HR. These results are best explained by a model in which an intact nicked site aligns with the repair template without being converted into a processed DSB. An end-processed DSB will align with both replacement and insertion templates without distinction, and accordingly we see no effect of the target site on DSB-induced HR (data in Figure 6, model in Figure 8). If nicks were converted to DSBs prior to alignment with the repair template, we would expect a similar result. The observed data can be explained, however, if intact nicks align with the repair template. A nicked template is asymmetric, so the model of repair with a single-stranded AAV template proceeds differently with a '+' or a '–' strand template. However, both orientations of nick repair generate a heterodimer between an intact target strand and intact template strand. This is not formed if both strands are cleaved. One hybridized target/template would generate a bulge, while the other would generate only mismatches, and we hypothesize that differential resolution of these two repair intermediates explains the observed differential HR activity.

Previous studies of HR using AAV templates in the absence of any endonuclease have shown that HR that removes an insert is less efficient than one with only mismatches (26). These data match the pattern we observed with nick-induced HR, suggesting that the mechanism of nick-induced HR may more closely reflect the mechanism of HR in the absence of endonucleases. In addition, it is relevant that many HR reporter systems have been designed to require removal of an inserted recognition site, which we would expect to yield an underestimate of the ability of nicks to induce HR.

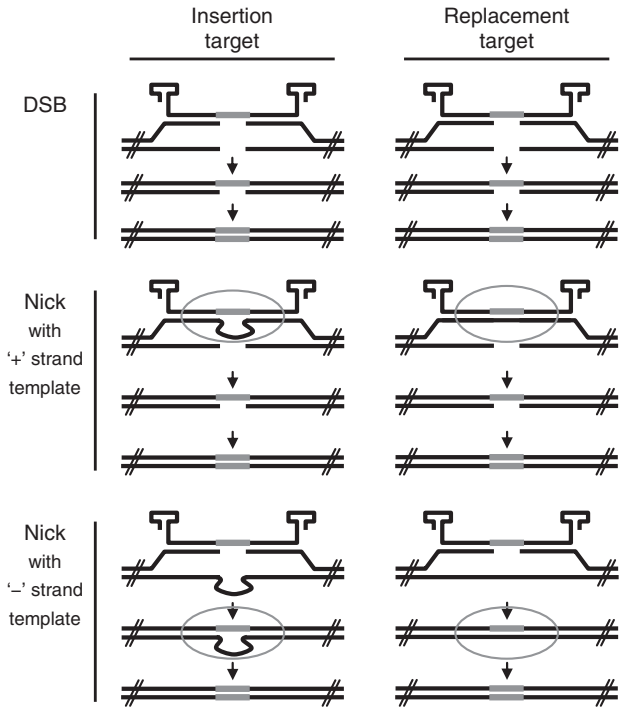

Figure 8. Model for HR at DSBs and nicks. When either the replacement or insertion target sites are cleaved, the ends will be processed and the AAV vector template will invade and align with one of the broken strands. When the replacement and insertion sites are nicked, however, the alignment of the target and AAV vector template is different. The nicked target can align with a single-stranded AAV vector template of either '+' or '–' orientation, followed by Holiday junction resolution and completion of HR. Notably, in nick-induced HR with either template there is a step in which an intact heterodimer is present (marked with a gray circle). This does not occur if both strands are cut. We hypothesize that the discordant activity observed in Figure 6 could be explained by discrimination at the level of resolution of this heterodimer.

It has been suggested that nicks could only stimulate HR upon conversion to DSBs, making nick-induced HR simply a less efficient version of DSB-induced HR; however, our results argue that nicks induce gene targeting by an uncharacterized mechanism that is distinct from the DSB-induced HR pathway. DSBs are acutely toxic and have the potential to generate oncogenic translocations, and a mechanism that induces HR without these side effects will be important for clinical applications of gene targeting.

SUPPLEMENTARY DATA

Supplementary Data are available at NAR Online.

ACKNOWLEDGEMENTS

We thank Dan Miller for his advice and discussions during this work and we thank both Dan Miller and David Russell for providing plasmids for foamy virus preparation, as well as the plasmid pCnZPNO and AAV template vector plasmid pA2nZ3113. We also thank Mike Certo and Andrew Scharenberg for the HA-tagged-I-AniIY2 expression plasmid and lentiviral plasmid, and Ryo Takeuchi for the purified I-AniIY2 cleavase used for *in vitro* assays.

FUNDING

National Institutes of Health UL1 DE19582, Pilot grant from the Northwest Genome Engineering Consortium (to M.J.M. and A.D.M.); P30 DK47754, Molecular Therapy Core Center grant (to A.D.M.); CA09229, training grant (to M.J.M.). Funding for open access charge: UL1 DE19582.

Conflict of interest statement. Two of the authors (B.L.S. and A.M.S.) are named inventors on a patent application entitled 'Generation of a DNA nicking enzyme that stimulates site-specific gene conversion from a homing endonuclease'. Other authors have declared no conflict of interest.

REFERENCES

1. Russell,D.W. and Hirata,R.K. (1998) Human gene targeting by viral vectors. *Nat. Genet.*, **18**, 325–330.
2. Miller,D.G., Wang,P.R., Petek,L.M., Hirata,R.K., Sands,M.S. and Russell,D.W. (2006) Gene targeting in vivo by adeno-associated virus vectors. *Nat. Biotechnol.*, **24**, 1022–1026.
3. Rouet,P., Smih,F. and Jasin,M. (1994) Expression of a site-specific endonuclease stimulates homologous recombination in mammalian cells. *Proc. Natl Acad. Sci. USA*, **91**, 6064–6068.
4. Urnov,F.D., Miller,J.C., Lee,Y.L., Beausejour,C.M., Rock,J.M., Augustus,S., Jamieson,A.C., Porteus,M.H., Gregory,P.D. and Holmes,M.C. (2005) Highly efficient endogenous human gene correction using designed zinc-finger nucleases. *Nature*, **435**, 646–651.
5. Miller,D.G., Petek,L.M. and Russell,D.W. (2003) Human gene targeting by adeno-associated virus vectors is enhanced by DNA double-strand breaks. *Mol. Cell. Biol.*, **23**, 3550–3557.
6. Porteus,M.H., Cathomen,T., Weitzman,M.D. and Baltimore,D. (2003) Efficient gene targeting mediated by adeno-associated virus and DNA double-strand breaks. *Mol. Cell. Biol.*, **23**, 3558–3565.
7. Petek,L.M., Russell,D.W. and Miller,D.G. (2010) Frequent endonuclease cleavage at off-target locations in vivo. *Mol. Ther.*, **18**, 983–986.
8. Kaykov,A. and Arcangioli,B. (2004) A programmed strand-specific and modified nick in S. pombe constitutes a novel type of chromosomal imprint. *Curr. Biol.*, **14**, 1924–1928.
9. Pauklin,S., Burkert,J.S., Martin,J., Osman,F., Weller,S., Boulton,S.J., Whitby,M.C. and Petersen-Mahrt,S.K. (2009) Alternative induction of meiotic recombination from single-base lesions of DNA deaminases. *Genetics*, **182**, 41–54.
10. Lee,G.S., Neiditch,M.B., Salus,S.S. and Roth,D.B. (2004) RAG proteins shepherd double-strand breaks to a specific pathway, suppressing error-prone repair, but RAG nicking initiates homologous recombination. *Cell*, **117**, 171–184.
11. Nakahara,M., Sonoda,E., Nojima,K., Sale,J.K., Takenaka,K., Kikuchi,K., Taniguchi,Y., Nakamura,K., Sumitomo,Y., Bree,R.T. *et al.* (2009) Genetic evidence for single-strand lesions initiating Nbs1-dependent homologous recombination in diversification of Ig v in chicken B lymphocytes. *PLoS Genet.*, **5**, e1000356.
12. Smith,G.R. (2004) How homologous recombination is initiated: unexpected evidence for single-strand nicks from V(D)J site-specific recombination. *Cell*, **117**, 146–148.
13. van Nierop,G.P., de Vries,A.A., Holkers,M., Vrijsen,K.R. and Gonçalves,M.A. (2009) Stimulation of homology-directed gene targeting at an endogenous human locus by a nicking endonuclease. *Nucleic Acids Res.*, **37**, 5725–5736.

14. Zhou,X., Zolotukhin,I., Im,D.S. and Muzyczka,N. (1999) Biochemical characterization of adeno-associated virus rep68 DNA helicase and ATPase activities. *J. Virol.*, **73**, 1580–1590.
15. Henckaerts,E., Dutheil,N., Zeltner,N., Kattman,S., Kohlbrenner,E., Ward,P., Clément,N., Rebollo,P., Kennedy,M., Keller,G.M. *et al.* (2009) Site-specific integration of adeno-associated virus involves partial duplication of the target locus. *Proc. Natl Acad. Sci. USA*, **106**, 7571–7576.
16. Landthaler,M., Lau,N.C. and Shub,D.A. (2004) Group I intron homing in Bacillus phages SPO1 and SP82: a gene conversion event initiated by a nicking homing endonuclease. *J. Bacteriol.*, **186**, 4307–4314.
17. Shen,B.W., Landthaler,M., Shub,D.A. and Stoddard,B.L. (2004) DNA binding and cleavage by the HNH homing endonuclease I-HmuI. *J. Mol. Biol.*, **342**, 43–56.
18. Niu,Y., Tenney,K., Li,H. and Gimble,F.S. (2008) Engineering variants of the I-SceI homing endonuclease with strand-specific and site-specific DNA-nicking activity. *J. Mol. Biol.*, **382**, 188–202.
19. McConnell Smith,A., Takeuchi,R., Pellenz,S., Davis,L., Maizels,N., Monnat,R.J. and Stoddard,B.L. (2009) Generation of a nicking enzyme that stimulates site-specific gene conversion from the I-AniI LAGLIDADG homing endonuclease. *Proc. Natl Acad. Sci. USA*, **106**, 5099–5104.
20. Trobridge,G., Vassilopoulos,G., Josephson,N. and Russell,D.W. (2002) Gene transfer with foamy virus vectors. *Methods Enzymol.*, **346**, 628–648.
21. Naldini,L., Blomer,U., Gage,F.H., Trono,D. and Verma,I.M. (1996) Efficient transfer, integration, and sustained long-term expression of the transgene in adult rat brains injected with a lentiviral vector. *Proc. Natl Acad. Sci. USA*, **93**, 11382–11388.
22. Halbert,C.L. and Miller,A.D. (2004) AAV-mediated gene transfer to mouse lungs. *Methods Mol. Biol.*, **246**, 201–212.
23. Takeuchi,R., Certo,M., Caprara,M.G., Scharenberg,A.M. and Stoddard,B.L. (2009) Optimization of in vivo activity of a bifunctional homing endonuclease and maturase reverses evolutionary degradation. *Nucleic Acids Res.*, **37**, 877–890.
24. Matthews,B.W. (2005) The structure of E. coli beta-galactosidase. *C. R. Biol.*, **328**, 549–556.
25. Thyme,S.B., Jarjour,J., Takeuchi,R., Havranek,J.J., Ashworth,J., Scharenberg,A.M., Stoddard,B.L. and Baker,D. (2009) Exploitation of binding energy for catalysis and design. *Nature*, **461**, 1300–1304.
26. Russell,D.W. and Hirata,R.K. (2008) Human gene targeting favors insertions over deletions. *Hum. Gene Ther.*, **19**, 907–914.